Article

Towards Zero Micro/Macro-Scale Wear Using Periodic Nano-Layered Coatings

Oleksiy V. Penkov, Alexander Yu. Devizenko, Mahdi Khadem,
Evgeniy N. Zubarev, Valeriy V. Kondratenko, and Dae-Eun Kim

ACS Publications

Towards Zero Micro/Macro-Scale Wear Using Periodic Nano-Layered Coatings

Oleksiy V. Penkov †, Alexander Yu. Devizenko ‡, Mahdi Khadem §, Evgeniy N. Zubarev ‡,

Valeriy V. Kondratenko ‡ and Dae-Eun Kim ‡§*

†Center for Nano-Wear, Yonsei University, Seoul 120-749, Korea

‡X-Ray Optics Lab, National Technical University "KhPI", Kharkiv 61002, Ukraine

§Department of Mechanical Engineering, Yonsei University, Seoul 120-749, Korea.

* Corresponding author. Email address: kimde@yonsei.ac.kr

ABSTRACT: Wear is an important phenomenon that affects the efficiency and life of all moving machines. In this regard, extensive efforts have been devoted to achieve the lowest possible wear in sliding systems. With the advent of novel materials in recent years, technology is moving towards realization of zero wear. Here, we report on the development of new functional coatings comprised of periodically stacked nanolayers of amorphous carbon and cobalt that are extremely wear resistant at the micro and macro scale. Because of their unique structure, these coatings simultaneously provide high elasticity and ultra-high shear strength. As a result, almost zero wear was observed even after one million sliding cycles without any

lubrication. The wear rate was reduced by 8~10-fold compared with the best previously reported data on extremely low wear materials.

1. INTRODUCTION

Wear occurs as a result of prolonged frictional interaction between two contacting surfaces in relative motion. Wear is often a critical issue in various industries including automotive, machinery, aerospace, biomedical, and electronic device.[1-3] Especially in micro-scale systems where liquid lubrication cannot be used due to high surface tension, wear remains as a great challenge that needs to be overcome to enable these systems to operate in dry contact conditions. Because wear significantly reduces the efficiency and life of any system that contains sliding parts, considerable efforts have been made to develop effective methods to eliminate wear to conserve resources and energy.

Various strategies have been developed for this purpose, including the use of hard and soft metallic coatings[4], diamond-like carbon (DLC) coatings,[5-7] chemical coatings,[8,9] graphene,[10] graphene oxide,[11] and micro- and nanocomposite coatings.[3,12] All these coatings have been successfully used to reduce friction and wear in various applications. Up to date, several researchers reported about achieving zero wear which was observed under certain sliding conditions for different materials, including DLC,[13] graphene,[14] and graphene oxide.[15] For example, Thorwarth et al. reported that after sliding tests performed using DLC coated implants,

no wear could be found but only local defects appeared on the surface.[13] Also, zero wear has been reported for nano-scale sliding systems. Peng et al. reported zero wear of mechanically exfoliated graphene nano sheets (MEGNS) when tested using an atomic force microscope (AFM).[14] The authors claimed that zero wear was due to fully elastic interaction at the contact region on the MEGNS specimen. As a result, the frictional energy was dissipated through an elastic rather than plastic process during the sliding test. Though these results suggested that extremely low wear may be achieved, the experimental conditions used in these works were rather limited in that either lubrication[16] was used, or the load as well as the number sliding cycles was insufficient.[13,14] In this regard, challenge still remains to demonstrate the feasibility of zero wear over extended sliding distance with sufficient load in dry conditions.

The advent of novel nanomaterials with superior mechanical and physical properties in recent years has opened new possibilities to achieve extremely low wear. The ability of nanomaterials to reduce wear at the macro-scale was observed several years ago.[17] For example, the use of several monolayers of graphene was found to significantly reduce friction and wear during the dry sliding of a steel ball across a copper plate.[18] Similar wear resistant behavior of graphene has also been reported for cases of sliding across steel plates or silicon wafers.[19,20]

Considering the benefits of single-layer coatings, combination of different layers could provide additional benefits because of their synergistic effects. For example, an additional interlayer can improve the adhesion between a substrate and a hard protective coating.[21] Commonly, the mechanism by which a multilayer coating can improve the friction and wear properties of a surface is dependent on the type of coating, the thickness of the individual layers, the number of layers and their order. Just using only two well-designed layers can yield a significant reduction in friction and wear.[22] The use of periodic multilayer coatings (PMC)

based on amorphous carbon and metal enables wear resistance comparable to that of DLC coatings.[23]

Table 1. Progress of lowest reported wear-rate values

Material/ Substrate	Atmosphere	Counter Interface	Contact Pressure [MPa]	Wear Rate [mm^3/N·mm]	Author	Year
Pt + N-doped DLC/ Silicon	ambient	Stainless Steel	~ 600	$1.9 \cdot 10^{-9}$	Khun & Liu[24]	2014
C$_{60}$ DLC/ Silicon	ambient	Silicon Nitride	~ 1100	$1.2 \cdot 10^{-11}$	Penkov et al.[22]	2013
DLC/ Polyether	ambient	Stainless Steel	~ 300	$3 \cdot 10^{-12}$	Kaczorowski et al.[26]	2014
Graphene/ Steel	H$_2$ atmosphere	Stainless Steel	~ 500	$2 \cdot 10^{-12}$	Berman et al.[20]	2014
Co-C multilayer/ Silicon	ambient	Stainless Steel	~ 700	**$< 3 \cdot 10^{-13}$**	Present work	

The wear resistance of various materials can be quantitatively compared by using a standard wear parameter such as the wear rate (WR). The wear rate can be calculated using the following equation:

$$WR = V/ (F \cdot L), \tag{1}$$

where V is the wear volume (mm^3), which is the amount of material removed from the surface during sliding; F is the normal force applied (N); and L is the sliding distance (mm). A compilation of extremely low wear rate values reported in recent years is provided in Table 1.[7,20,22,24-26] Currently, a wear rate of $2 \cdot 10^{-12}$ mm^3/N·mm is the lowest reported value, which was achieved with a steel ball sliding against graphene in a hydrogen atmosphere.[20]

In this work, we report on the development of a new functional coating that is comprised of alternating nanolayers of amorphous carbon and cobalt that exhibit extraordinarily high micro and macro scale wear resistance without any lubrication and under ambient conditions. The wear rate of our functional coating was 8~10-fold lower than that of the lowest value reported up to date.

2. EXPERIMENTAL METHODS AND MATERIALS

In this section, we specify the materials, fabrication, and characterization techniques that are used for this work.

2.1 Fabrication. The Co/C (PMCs) and single-layer coatings were prepared by a dual DC magnetron sputtering process in an argon atmosphere. The coatings were deposited onto polished Si (111) wafers with an area of 1x1 cm^2. Graphite (99.99%) and cobalt (99.999%) targets with a diameter of 100 mm were used. The base pressure before the deposition was about 10^{-3} Pa. Before deposition, the surface of the wafer was cleaned by an ion beam (U=1000

V, I = 7 mA). The argon pressure during deposition was maintained at 0.22 Pa. The thickness of the individual layers was controlled by adjusting the exposure time. The substrate temperature was maintained below 50°C during the sputtering process. The deposition rates were about 0.14 and 0.3 nm/s for carbon and cobalt, respectively.

2.2 Structure and property evaluation. The microstructure of the coatings was evaluated using TEM (JEOL JEM-ARM200F). The structure of the carbon layers was analyzed by Raman spectroscopy (JY Horiba Labram Aramis), and the surface roughness and wear were characterized by AFM (Park Systems NX 10) and high-resolution 3D Laser Microscopy (Keyence VK-X210). The mechanical properties of the coatings were evaluated using a high-precision ultra-nano hardness tester (CSM, UNHT).[27,28] Two different types of diamond indenters were used for the hardness measurements. The first one was a Berkovich pyramid having a rounded end with a diameter of 100 nm. The second indenter was a hemispherical tip with a radius of 200 μm.

2.3 Friction and wear evaluation. The friction and wear behaviors were investigated by using a custom-built reciprocating tribotester. All experiments were performed under ambient conditions at a temperature of ~25ºC and a relative humidity of 45–50% in a Class 100 clean room. The sliding speed was 10 mm/s with a stroke of 2 mm, which resulted in a sliding frequency of 2.5 Hz. Stainless steel balls of 1 mm in diameter were used as the counter surface. To ensure the repeatability of the experimental data, at least three sliding tests were performed for each experimental condition, and a new pin was used for each experiment. The normal load was in the range of 10–100 mN. The number of sliding cycles was varied depending on the wear resistance of the samples.

2.4 FEM Simulations. The FEM simulations were performed by using a commercial software COMSOL 5.1 in 2D mode. The elastic, plastic and creep behaviors were incorporated in the analyses. The actual structure of the coatings (the thickness and number of Co/C layers) was used in the model. For further details, see the Supplementary Information.

3. RESULTS AND DISCUSSION

In this section, we first describe the design process of the functional coatings for ultra-low wear. Then, structural characterization, friction and wear behavior are assessed. Finally, we propose the mechanism of ultra-low wear, which is based on the results of FEM simulations.

3.1 Design of the functional coatings. The basic concept underlying the design of these new functional coatings is based on the compilation of existing knowledge regarding the mechanisms of friction and wear reduction.[29-32] We attempt to achieve a synergistic effect through the combination of three basic concepts. The first is the use of highly elastic materials such as polymers. Polymers exhibit low wear because of their effective damping, especially at relatively high sliding rates.[32,33] The second concept is the use of hard materials with high shear strength that promote wear reduction by mitigating the effects of ploughing and tearing.[29] However, the negative aspect of such a high shear strength material is that friction can be high if the asperities on the contacting surfaces interlock during sliding.[31] To overcome this issue, a high shear strength material can be coated with a thin layer of a low shear strength material to reduce the friction; this is the third concept that we incorporate in the design of the functional coating. Typically, materials such as graphene or MoS_2 are used for this purpose.[31] The first and second concepts were partially implemented in our previous research on bi-layer Si/C tribological coatings,[22] in which the combination of two amorphous materials with different

mechanical properties enabled a significant reduction in macro-scale wear using only two layers with thicknesses of 20–100 nm. In that case, the friction and wear were reduced because of the ability of the coating to elastically deform under the applied load. However, the applicability of this coating was limited because of the high stiffness of silicon, which resulted in a rapid increase in wear with increasing load. It seemed reasonable that the elasticity of such a coating can be enhanced by increasing the number of layers and using a material that is less stiff than silicon.

In order to develop a new coating with extremely low wear characteristics several major parameters need to be determined, such as the deposition method, the type of materials and the desired structure, which implies the order, number and thickness of the layers. In this work sputtering process was chosen because it allows for the deposition of a variety of materials onto various substrates. Sputtering is also suitable for industrial applications and provides high productivity and scalability.

It was desirable that the materials used in the coating be amorphous because amorphous materials exhibit higher elasticity compared with their polycrystalline counterparts.[34] First, carbon was selected as the material for the soft layer because its potential for reduction of friction and wear has been already demonstrated.[22, 23] The second material was selected based on the following criteria: limited intermixing with carbon; an amorphous structure; the ability to form a nanometer-thick continuous layer during deposition by sputtering; and a high hardness and Young's modulus. Based on these criteria, cobalt was selected as the material for the second layer.

It has been known that an extremely thin layer of cobalt deposited on carbon by sputtering exhibits an amorphous structure.[35,36] It was found that when the thickness of the layer exceeded

~4 nm, crystallization of the cobalt occurred. Thus, to maintain the amorphous cobalt structure, its thickness should be below ~4 nm. Therefore, an initial thickness of 3 nm was selected for the cobalt layers. The initial thickness of the carbon layers was selected to be slightly higher (4 nm). The number of layers in the coatings was determined by the total thickness of the coating. The total thickness was limited by the internal stress generated during the sputtering process.[37] Based on our previous experience, the overall coating thickness of about ~200 nm was considered to be adequate. For cobalt and carbon layer thicknesses of approximately 3 and 4 nm, respectively, 200 nm corresponded to 36 pairs of carbon and cobalt layers. To determine the optimal structure of the coating, the thicknesses were varied from 4 to 19 nm for carbon and from 1.5 to 5.6 nm for cobalt. The specifications of the PMC samples used in this work are listed in Table 2.

Table 2. List of PMC specimens used in the experiments

| Sample name	Layer thickness [nm]		Number of Co/C layers
	Cobalt	Carbon	
1.5/4	1.5	4.0	37
2/4	2.0	4.0	5, 10, 20, 36
3/4	3.0	4.0	29
3.8/4	3.8	4.0	25
5/4	5.6	4.0	20

2/8	2.0	8.0	21
2/12	2.0	12.0	15
2/16	2.0	16.0	10
2/19	2.0	19.2	8

3.2 Structural and mechanical properties of the coatings. The PMC comprised of alternating layers of carbon and cobalt. The material of bottom and top layers was carbon. This configuration was selected to improve the adhesion between the coating and the substrate and to provide a low friction layer on the surface. Moreover, the top carbon layer served to protect the cobalt layers from oxidation. The surface roughness was approximately 1 nm (R.M.S.) for all the samples.

Cross-sectional transmission electron microscopy (TEM) images of several Co/C PMCs are presented in Figure 1. The thicknesses of the individual layers measured using TEM precisely matched the values calculated from the low-angle X-ray diffraction (LAXRD) data. The amorphous structure of the carbon was also confirmed using Raman spectroscopy (Figure 2). As shown in the Raman spectra, absolute intensity of the Raman peak for the multilayer coating was approximately 40% lower compared with that of the single-layer coating. This difference was attributed to the lower amount of carbon in the multilayer coating. Nevertheless, the width and relative intensities and positions of the D and G components of the peak were almost identical. This revealed that the microstructure of the carbon in the single-layer and multilayer coatings was the same.

When the thickness of the cobalt layers exceeded ~3.5 nm, partial crystallization of the cobalt occurred and became visible in the TEM images. Dark regions in the diffraction contrast appeared inside the cobalt layers (Figure 1c). High-magnification imaging of these areas enabled the direct observation of the crystalline planes of the cobalt, which were parallel to the substrate (inset in Figure 1c).
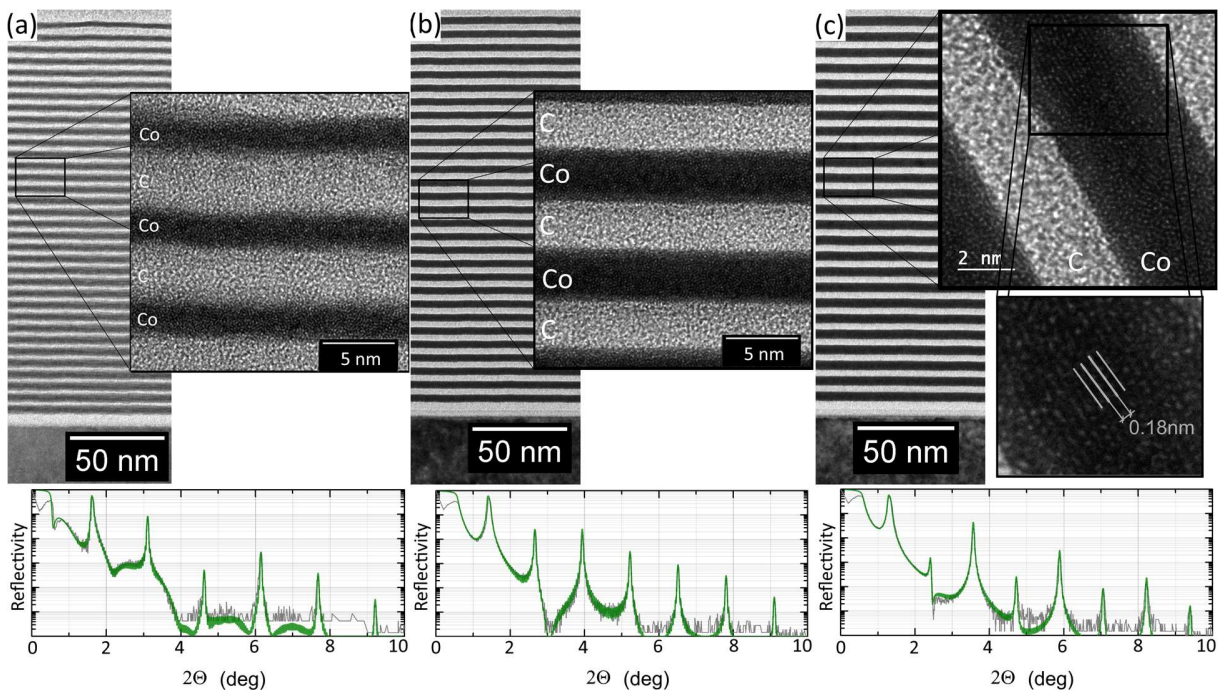
Figure 1. Structure of Co/C PMCs. Cross-sectional TEM images and LAXRD curves of samples with cobalt/carbon layers of the following thicknesses: (a) 2/4, (b) 3/4 and (c) 3.8/4 nm.

The mechanical properties of the coatings were assessed using the ultra-nano hardness testing (UNHT) method.[27] First, the indentation hardness and Young's modulus were determined using a Berkovich pyramidal tip (Figure 3a and 3b). With the carbon thickness fixed at 4 nm, the indentation hardness and Young's modulus initially increased with increasing cobalt thickness and crystallization (Figure 3a). The hardness decreased when the cobalt thickness exceeded 3.5 nm. This decrease was attributed to the structural changes in the cobalt layer that occurred at

the beginning of crystallization. By contrast, the Young's modulus increased after crystallization. With the cobalt thickness fixed at 2 nm, increasing the carbon thickness led to a monotonic reduction in both hardness and modulus, as expected (Figure 3b). This reduction was attributed to the increasing portion of carbon, which was much softer.

The second set of indentations was performed using a hemispherical diamond tip with a radius of 200 μm. The data obtained from these measurements were used to construct and verify the FEM model. The indentation behavior of the PMC was compared with that of the bare silicon substrate and that of a single-layer carbon coating. Typical experimental and simulated loading–unloading curves for the PMCs that were tested with the hemispherical indenter are presented in Figure 3c. The simulated results matched the experimental ones almost perfectly. The PMCs with amorphous cobalt exhibited pure elastic deformation. No plastic deformation or creep was observed.

As the cobalt structure transformed into a nanocrystalline structure with increasing thickness, the behavior of the indentation curve also changed significantly. Under the same indentation conditions, the coating with nanocrystalline cobalt deformed plastically. The creep was also significant in this case (Figure 3c). The value of the yield strength obtained by the FEM simulation for nanocrystalline cobalt was approximately 100 MPa.

Nano-indentation measurement results showed that the elastic deformation behavior of the coatings depended on the carbon thickness (Figure 3d). In the case of low carbon thickness, the nano-indentation behavior was almost the same as that of the bare silicon substrate. Increasing the carbon content led to an increase in the elastic deformation of the coating, which approached the value for a single-layer carbon coating of the same total thickness. Thus, the elastic

deformation of the PMCs was determined to be between the elastic deformation of the silicon substrate and the elastic deformation of the single-layer carbon coating, as indicated by the horizontal lines in Figure 3d.
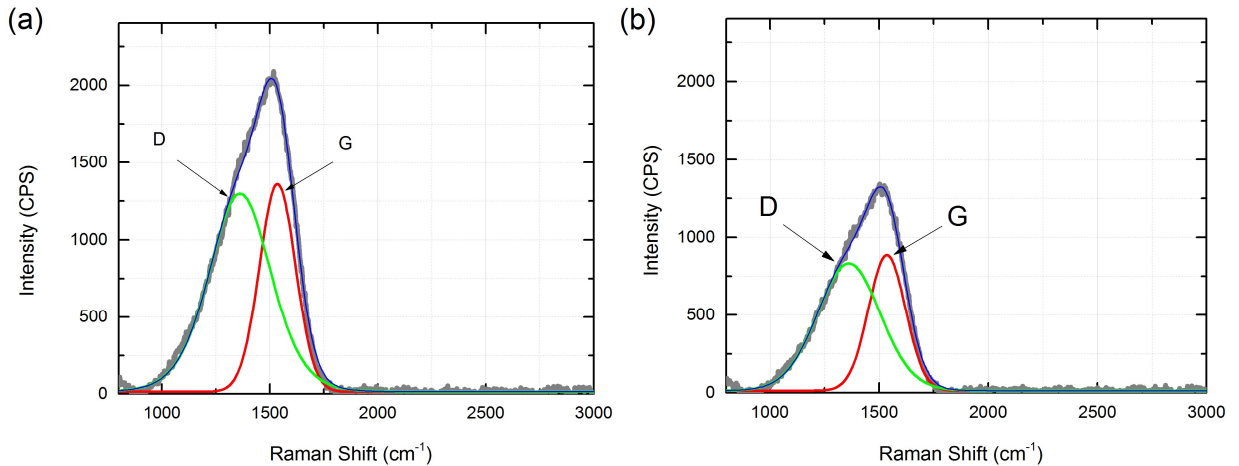

Figure 2. Raman spectroscopy data. D and G peaks of carbon for excitation wavelength of 532 nm for (a) 220 nm thick single layer carbon coating and (b) PMC 2/12.

3.3 Frictional properties. The frictional and wear characteristics of the coatings were assessed using a reciprocating tribotester. Variations in the friction coefficient with respect to the number of sliding cycles for three different tests are shown in Figure 4a. As observed, the friction coefficient was quite repeatable and remained very stable for more than 1 million sliding cycles under a normal load of 20 mN. This large number of sliding cycles resulted in a wear track of only 10 nm in depth (Figure 4b). Coatings with various thicknesses of cobalt and carbon exhibited very similar friction coefficient values in the range of 0.08–0.12.

The amount of wear was calculated based on the volume of material removed from the surface after a certain number of sliding cycles. The wear volume was calculated by measuring the cross-sectional area of the wear track by using a 3D laser microscope and multiplying this value by the length of the wear track. Several examples of wear track cross-sections are shown in

Figure 4c. The wear resistance of the PMCs was observed to be significantly affected by the thickness of the carbon and cobalt layers.
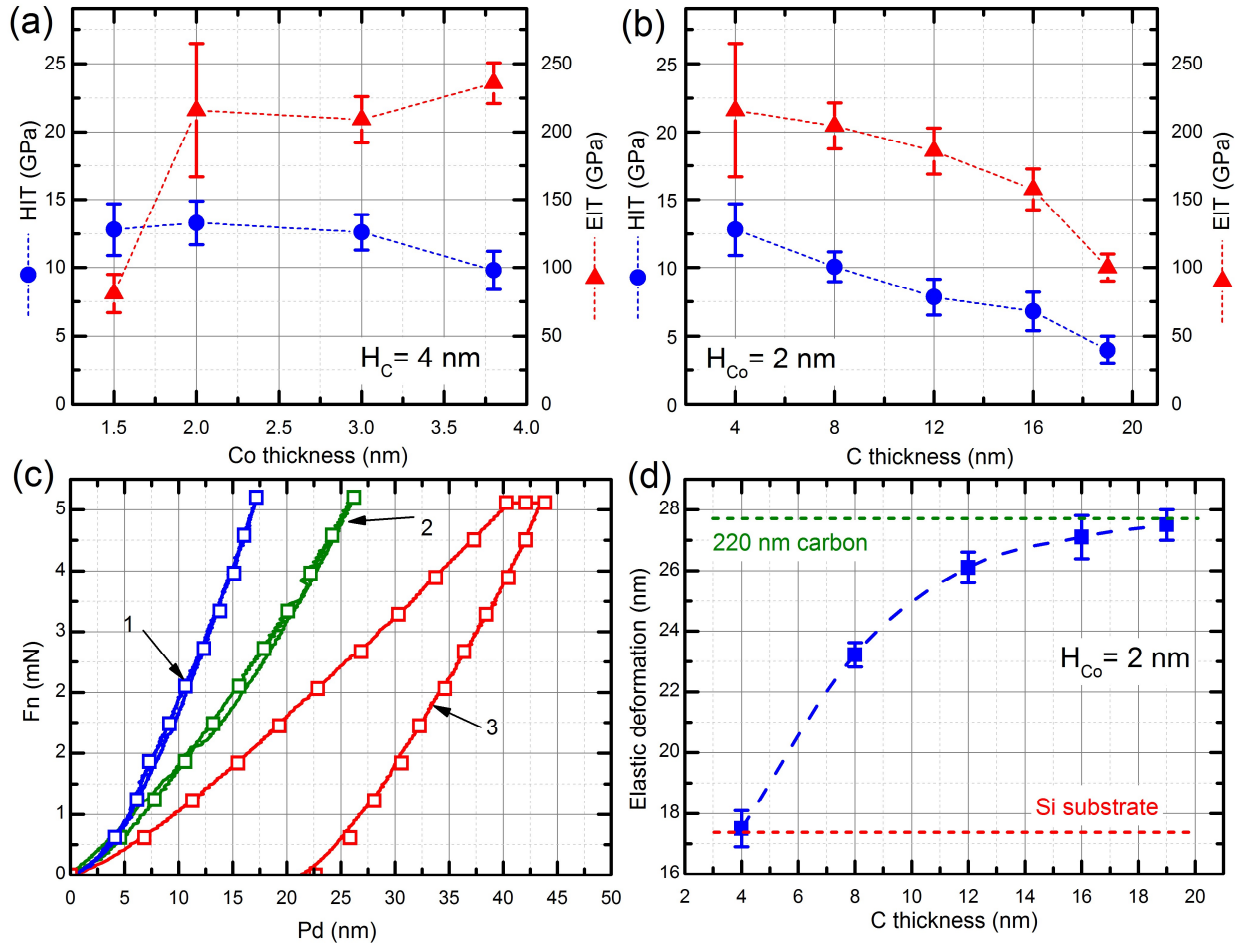
Figure 3. Mechanical properties of the PMCs. Indentation hardness and Young's modulus as functions of (a) the cobalt thickness and (b) the carbon thickness. (c) Force–displacement curves for various PMCs during indentation with a 200 µm spherical indenter: 1 – 2/4; 2 – 2/12; 3 – 3.8/4 (solid lines- experiment, squares – FEM simulation). (d) Elastic deformation of the PMCs as a function of the carbon thickness for a fixed cobalt thickness of 2 nm.

Increasing the cobalt thickness from 1.5 nm to 2 nm led to a decrease in the wear rate from $5 \cdot 10^{-12}$ mm³/N·mm to $1.5 \cdot 10^{-12}$ mm³/N·mm (Figure 5a). No significant difference in the wear rate was observed between the samples with cobalt thicknesses of 2 and 3 nm. It was postulated

that the coatings with very thin cobalt layers (1.5 nm) exhibited higher wear because the small amount of cobalt was unable to improve the overall mechanical properties of the coatings. This hypothesis was consistent with the measured values of hardness and Young's modulus of the samples with different cobalt thickness (Figure 3a). The coatings with cobalt thicknesses of 2 and 3 nm exhibited nearly the same wear resistance. Further increase in the cobalt thickness to 3.8 nm drastically increased the wear rate to $4 \cdot 10^{-11}$ mm^3/N·mm. This phenomenon was attributed to the transformation of the structure of the cobalt layers from amorphous to nanocrystalline, and the resulting significant change in the mechanical properties of the coatings (Figure 3a). Further increase in the cobalt thickness slightly reduced the wear rate as a result of the improvement in the structure of the cobalt layers and the enhancement of their mechanical properties. However, the wear rate was still much higher compared with that observed in the case of amorphous cobalt layers. Thus, the experimental data indicated that the optimal thickness of the cobalt layers was in the range of 2–3 nm.

The variation of the carbon thickness for a fixed cobalt thickness also affected the wear rate significantly (Figure 5b). Initially, the wear rate decreased to $3 \cdot 10^{-13}$ mm^3/N·mm as the carbon thickness was increased from 4 to 12 nm. Further increase in the carbon thickness to 16 nm led to a drastic increase in the wear rate by 20-fold. Thus, the optimal carbon thickness was determined to be 12 nm. For given thicknesses of the cobalt and carbon layers, it was found that the number of Co/C layers significantly affected the wear rate of the PMC. As could be seen from Figure 5c for the case of the PMC 2/4, decrease in the number of the layers from 36 to 5 increased the wear rate by almost two orders of magnitude.

The wear rate depended on the normal load that was applied (Figure 5d). The lowest value of the wear rate, $3 \cdot 10^{-13}$ mm^3/N·mm, was measured at a normal load of 30 mN for the sample

2/12. This load corresponded to a nominal contact pressure of 700 MPa which was estimated by Hertzian contact theory.[38] For tests performed below 30 mN normal load wear was too small to be detected. Increasing the applied normal load from 30 to 100 mN led to an increase in the wear rate to $1.5 \cdot 10^{-12}$ mm^3/N·mm. This value was still less than the previously reported results for highly wear resistant materials (Table 1).
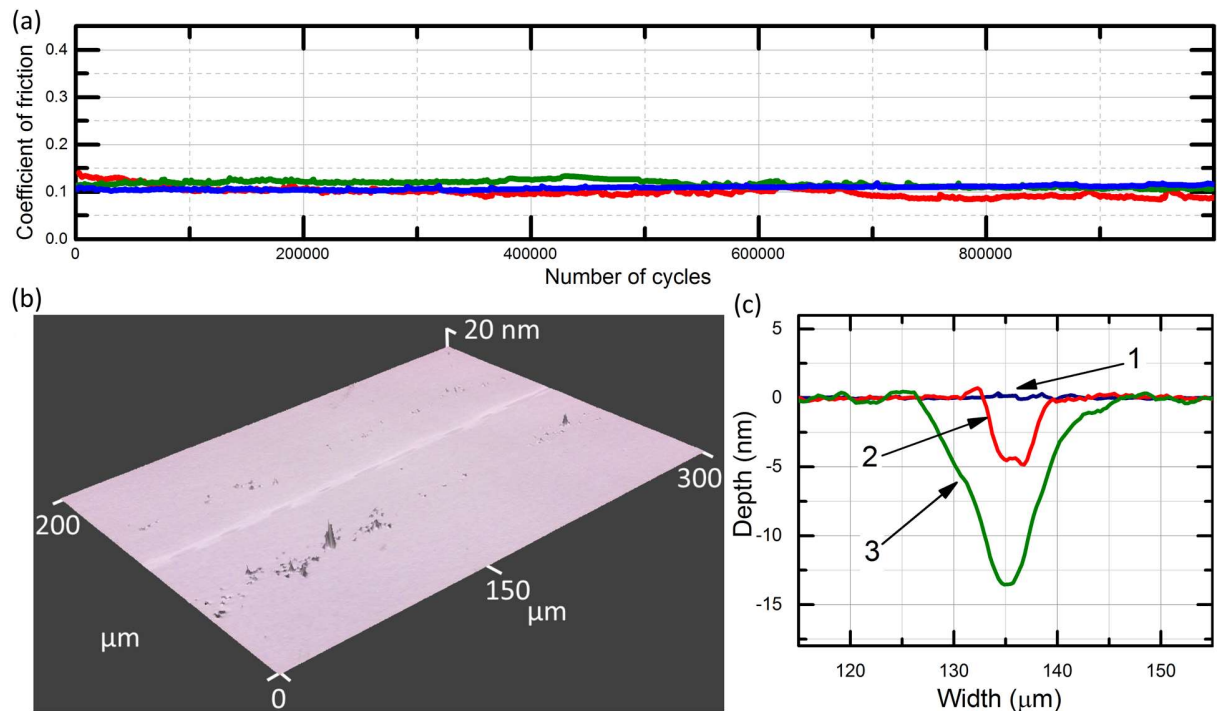
Figure 4. Friction and wear behavior of Co/C PMCs. (a) Friction coefficient as function of the sliding distance for three different tests and (b) 3D image of the wear track after 1 million sliding cycles under a load of 20 mN for the sample 2/12. (c) Variation in the profile of the wear track for various samples after 400,000 sliding cycles under a load of 20 mN: 1 – 2/12; 2 – 2/4; 3 – 3.8/4.

As for the stainless steel ball counter surface, no wear could be detected after the sliding test even when high-resolution surface characterization tools were used to carefully examine the surface of the ball (Supporting Data 3). The reason for this outcome may be explained by the fact that the stainless steel ball was significantly harder than the top carbon layer of the PMC.

Thus one may expect that there would be relatively less (or possibly no) wear incurred on the ball as it slides against the PMC surface. Also, due to the large elastic deformation of the coating under an applied normal load, the real area of contact between the ball and the PMC specimen increased which led to the decrease in the contact pressure (Fig. 3d). The low contact pressure was presumed to be less than the yield point of the stainless steel. In summary, the 2/12 PMC resulted in the lowest wear rate ever reported at micro/macro-scale with no wear incurred on the counter surface. It should be noted that such a low wear rate was achieved even without lubrication and in ambient conditions.
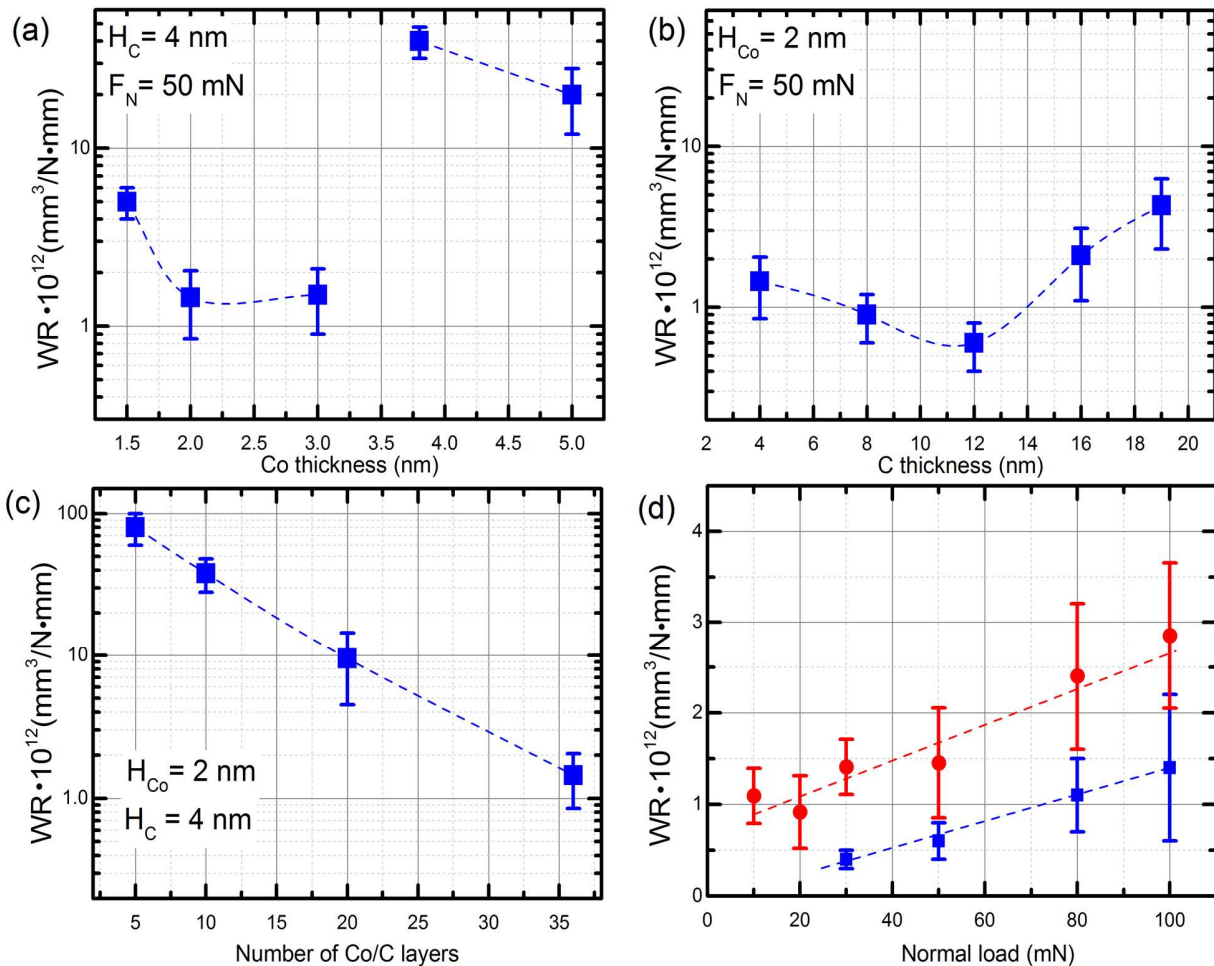
**Figure 5.** Wear behavior of Co/C PMCs. Wear rate as a function of (a) the thickness of the Co layers with the carbon thickness fixed at 4 nm and (b) the thickness of the carbon layers with the cobalt thickness fixed at 2 nm. (c) Wear rate as a function of the number of Co/C layers for the sample 2/4. (d) Wear rate as a function of the normal load for the samples 2/4 (red circles) and 2/12 (blue squares).

3.4 Mechanism of wear. FEM simulation was performed to understand the mechanism of the extremely low wear properties of the PMCs. The underlying design concept for the development of a low wear coating is based on the synergistic effects of its elastic and shear strength properties. This can be described in terms of the effective elastic and shear moduli of the coatings. These parameters were computed based on the FEM simulations. The effective elastic modulus is the ratio of the compressive stress to the elastic strain generated under loading by the counter surface (ball). The effective elastic modulus describes the ability of the coating to deform elastically. Thus, a lower modulus allows higher elastic deformation under a given load. An example of a simulation result of such a loading and the corresponding deformation of the individual layers in the coating is presented in Figure 6a.

After the loading (Figure 6a), a lateral force in the x-direction was applied, leading to surface shear and the generation of shear stress. The effective shear modulus is the ratio of the shear stress to the shear strain. The shear modulus describes the ability of a material to withstand lateral deformation. An example of the shear stress distribution calculated for the sample 2/12 is presented in Figure 6b. In the PMC, the shear stress was located near the contact point on the top carbon layer (dark red spot), whereas in the single-layer carbon coating, the shear stress was distributed over a much greater depth. Additionally, in the PMC, the stress was distributed along the x-axis in the cobalt layers. This stress distribution appears as light blue horizontal stripes of 2 nm in width in the figure. From the overall results of the FEM simulation, it can be concluded that the presence of relatively hard and stiff metallic interlayers significantly increased the shear strength of the coatings because of their orientation, which was parallel to the direction of the shear. Furthermore, FEM analysis of the contact stress at the interface of the steel ball and PMC showed that the stress generated in the ball was lower than the yield strength of the stainless

steel (Figure 6d). Based on this analysis, plastic deformation of the ball was not likely to occur which supported the experimental finding in which wear could not be detected on the ball after the sliding test.
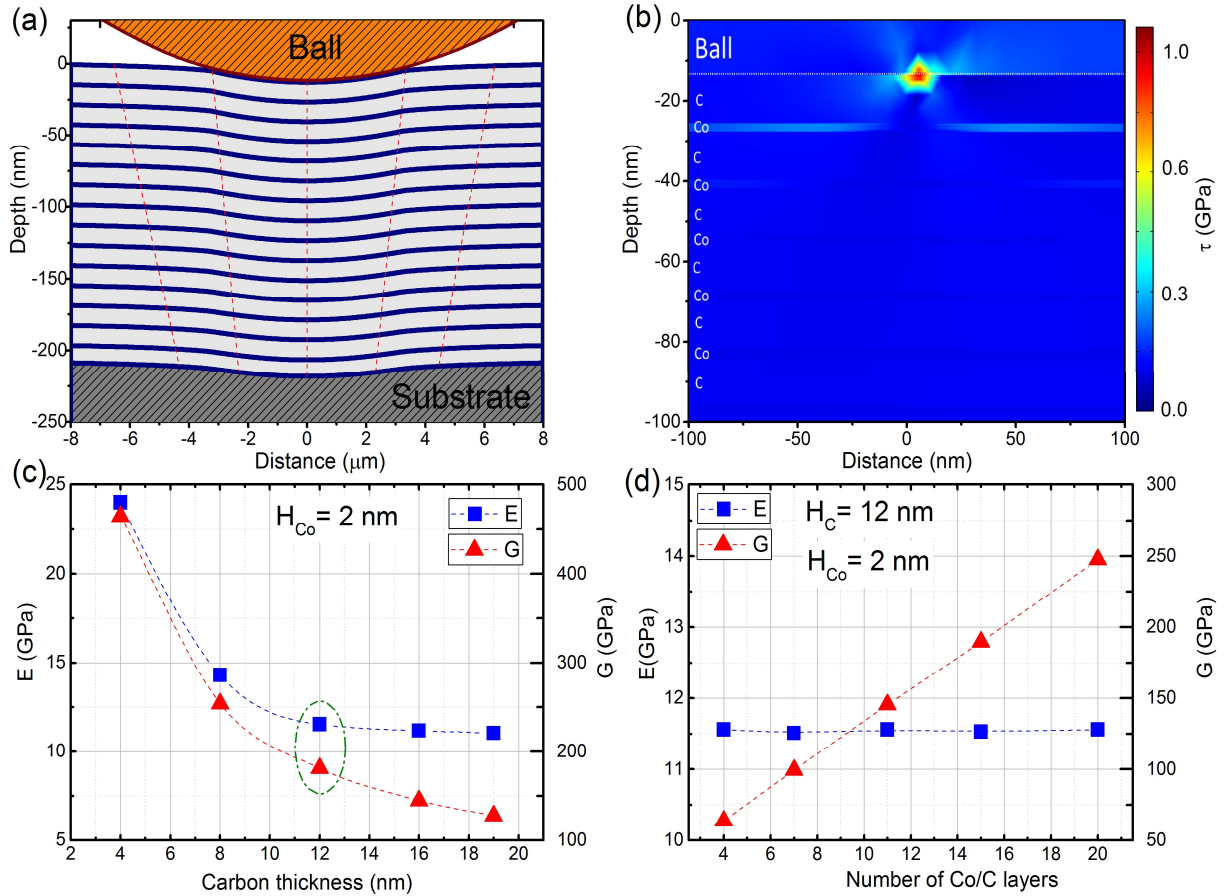
Figure 6. FEM simulation of contact between PMSc and a counter surface (ball). (a) Elastic deformation behavior of the PMC under a normal load of 50 mN and (b) the shear stress distribution in the PMC after the application of a lateral force on the counter surface under the same normal load. Calculated effective elastic (squares) and shear (triangles) moduli as functions of (c) the thickness of the carbon layers with a 2 nm cobalt thickness and (d) the number of Co/C pairs for fixed Co and C thicknesses of 2.0 nm and 12.0 nm, respectively.

The FEM simulation revealed that the effective elastic and shear moduli are significantly affected by the structure of the coating (Figure 6c and 6d). When the carbon thickness was low, the coating showed very high effective elastic and shear moduli. Experimental results

demonstrated that such coatings had moderate wear resistance (Figure 5b). When the carbon thickness was increased, both moduli were reduced. This meant that the shear strength decreased but the elasticity increased at the same time. When the carbon thickness increased from 4 to 12 nm, the elastic modulus decreased by 2-fold, but when the thickness was further increased from 12 to 19 nm, the elastic modulus varied only slightly. On the other hand, the shear modulus decreased significantly as the carbon thickness increased from 12 to 19 nm. Thus, the coatings with 12 and 19 nm thick carbon layers had almost the same elasticity, but the shear strength of the coating with 19 nm thick carbon layer was much lower.

By comparison of FEM results (Figure 6c) to the experimental data (Figure 5b), it could be concluded that increasing the elasticity of the coating increased the wear resistance as long as the effective shear modulus was higher than ~180 GPa. Decrease in the effective shear modulus below this level led to drastic decrease in the wear resistance. Among the various PMCs, the coating with cobalt/carbon thickness of 2/12 nm provided the optimum elastic and shear properties to achieve the highest wear resistance.

The FEM simulation results revealed that for coatings with a fixed layer thickness, increasing the number of layers (Figure 6d) had no effect on the effective elastic modulus of the PMC. This outcome was considered to be due to fact that the effective modulus of a composite coating generally depends on the modulus and ratio of the individual components. Thus, as long as the ratio of the individual components in a single Co/C layer does not change with increasing number of layers, the effective modulus of the multilayer coating should remain the same.

On the contrary, increasing the number of layers significantly increased the effective shear modulus of the PMC. This may be explained by the degree of shear displacement at the surface of the PMC for a given level of shear stress with respect to the number of layers. Since shear

modulus is defined as the shear stress divided by the shear strain, the shear modulus would increase with decreasing shear strain for a given shear stress. On the other hand, the shear strain is defined as shear displacement at the surface divided by the coating thickness. Thus, the fact that the effective shear modulus increased with the number of layers suggested that the shear strain decreased with increasing number of layers. From the FEM simulation, it was found that the shear displacement at the surface of the coating did not vary significantly with respect to the number of layers for a given shear stress. Hence, since the coating thickness increased with increasing number of layers, the effective shear strain decreased. In summary, since the shear strain decreased with increasing number of layers, the effective shear modulus increased.

From the results of the FEM simulations it was revealed that for coatings with a fixed layer thickness, increasing the number of layers had no effect on the elasticity but significantly increased the effective shear modulus. This outcome suggested that increasing the number of layers for a given thickness of individual layers appears to be a good strategy for reducing wear. This strategy was supported by the experimental data for the PMC 2/4 specimen shown in Figure 5c. From the practical point of view, the total number of layers should be limited by the total thickness, which in turn should be determined based on the capability of the deposition process.

4. CONCLUSIONS

This study is concerned on the development of new functional coatings comprised of periodically stacked nanolayers of amorphous carbon and cobalt that are extremely wear resistant at the micro/macro-scale. Our experimental results indicate that the wear resistance of well-designed functional multilayer coatings exceeds one of commonly used solid lubricants.

FEM simulations showed that PMC's simultaneously provide high elasticity and ultra-high shear strength due to their unique structure leading to extraordinary low wear rate of $3 \cdot 10^{-13}$ mm^3/N·mm that is 8~10-fold lower compare to the lowest reported values for DLC,[26] or single-layer graphene.[20]

ASSOCIATED CONTENT

Supporting information:

The supporting information provides additional details of the friction and wear tests, wear quantification and the FEM simulation methods. Also, the mechanism of cobalt crystallization, additional ultra-nano hardness test results and finite-element modeling simulation data are provided. This material is available free of charge via the Internet at http://pubs.acs.org

AUTHOR INFORMATION

Corresponding Author

*E-mail: kimde@yonsei.ac.kr

Author Contributions

The manuscript was written through contributions of all authors. All authors have given approval to the final version of the manuscript.

ACKNOWLEDGEMENT

ABBREVIATIONS

PMC, periodic multilayer coating; DLC, diamond-like carbon; LAXRD, Low-angle X-ray diffraction; TEM, Transmission electron microscopy; FEM, Finite element method.

REFERENCES

(1) Holmberg, K., Andersson, P., Nylund, N.O., Makela, K., Erdemir, A. Global energy consumption due to friction in trucks and buses. *Tribol. Int.* **2014**, *78*, 94-114.

(2) Woo, Y., Kim, S.H. Sensitivity analysis of plating conditions on mechanical properties of thin film for MEMS applications. *J. Mech. Sci. Technol.* **2011**, *25*, 1017-1022.

(3) Ramakrishna, S., Mayer, J., Wintermantel, E., Leong, K.W. Biomedical applications of polymer-composite materials: a review. *Compos. Sci. Technol.* **2001**, *61*, 1189-1224.

(4) Holmberg, K., Ronkainen, H., Matthews, A. Tribology of thin coatings. *Ceram. Int.* **2000**, *26*, 787-795.

(5) Grill, A. Diamond-like carbon coatings as biocompatible materials—an overview. *Diam. Relat. Mater.* **2003**, *12*, 166-170.

(6) Dearnaley, G., Arps, J.H. Biomedical applications of diamond-like carbon (DLC) coatings: A review. *Surf. Coat. Technol.* **2005**, *200*, 2518-2524.

(7) Penkov, O.V., Pukha, V.E., Zubarev, E.N., Yoo, S.S., Kim, D.E. Tribological properties of nanostructured DLC coatings deposited by C60 ion beam. *Tribol. Int.* **2013**, *60*, 127-135.

(8) Sung, I.H., Kim, D.E. Surface Damage Characteristics of Self-Assembled Monolayers of Alkanethiols on Metal Surfaces. *Tribol. Lett.* **2004**, *17*, 835-844.

(9) Chen, X., Kato, T., Nosaka, M. Origin of Superlubricity in a-C:H:Si Films: A Relation to Film Bonding Structure and Environmental Molecular Characteristic. *ACS App. Mater. Interface.* **2014**, *6*, 13389-13405.

(10) Penkov, O.V., Khadem, M., Lim, W.S., Kim, D.E. A review of recent applications of atmospheric pressure plasma jets for materials processing. *J. Coat. Technol. Res.* **2015**, *12*, 225-235.

(11) Liang, H., Bu, Y., Zhang, J., Cao, Z., Liang, A. Graphene Oxide Film as Solid Lubricant. *ACS App. Mater. Interface.* **2013**, *5*, 6369-6375.

(12) Khetan, V., Valle, N., Duday, D., Michotte, C., Mitterer, C., DelplanckeOgletree, M.P., Choquet, P. Temperature-Dependent Wear Mechanisms for Magnetron-Sputtered AlTiTaN Hard Coatings. *ACS App. Mater. Interface.* **2014**, *6*, 15403-15411.

(13) Thorwarth, K., Jaeger, D., Figi, R., Stiefel, M., Weisse, B., Muller, U., Thorwarth, G., Hauert, R. Near zero wear of diamond like carbon coated implants for up to 100 years of articulation. *European Cells Mater.* **2014**, *28*, 38-38.

(14) Peng, Y., Wang, Z., Zou, K. Friction and Wear Properties of Different Types of Graphene Nanosheets as Effective Solid Lubricants. *Langmuir* **2015,** *31,* 7782-7791.

(15) Mungse, H.P., Khatri, O.P. Chemically Functionalized Reduced Graphene Oxide as a Novel Material for Reduction of Friction and Wear. *J. Phys. Chem. C* **2014**, *118*, 14394-14402.

(16) Banerji, A., Edrisy, A., Francis, V., Alpas, A.T. Effect of bio-fuel (E85) addition on lubricated sliding wear mechanisms of a eutectic Al–Si alloy. *Wear* **2014**, *311*, 1-13.

(17) Penkov, O.V., Kim, H.J., Kim, H.J., Kim, D.E. Tribology of Graphene: A Review. *Int. J. Precis. Eng. Man.* **2014**, *15*, 577-585.

(18) Won, M.S., Penkov, O.V., Kim, D.E. Durability and degradation mechanism of graphene coatings deposited on Cu substrates under dry contact sliding. *Carbon* **2013**, *54*, 472-481.

(19) Berman, D., Erdemir, A., Sumant, A.V. Reduced wear and friction enabled by graphene layers on sliding steel surfaces in dry nitrogen. *Carbon* **2013**, *56*, 167-175.

(20) Berman, D., Deshmukh, S.A., Sankaranarayanan, S.K., Erdemir, A., Sumant, A.V. Extraordinary Macroscale Wear Resistance of One Atom Thick Graphene Layer. *Adv. Funct. Mater.* **2014**, *24*, 6640-6646.

(21) Takeno, T., Sugawara, T., Miki, H., Takagi, T. Deposition of DLC film with adhesive W-DLC layer on stainless steel and its tribological properties. *Diam. Relat. Mater.* **2009**, *18*, 1023-1027.

(22) Penkov, O.V., Bugayev, Y., Zhuravel, I., Kondratenkov, V.V., Amanov, A., Kim, D.E. Friction and Wear Characteristics of C/Si Bi-layer Coatings Deposited on Silicon Substrate by DC Magnetron Sputtering. *Tribol. Lett.* **2012**, *48*, 123-131.

(23) Yang, S., Teer, D.G. Investigation of sputtered carbon and carbon/chromium multi-layered coatings. *Surf. Coat. Technol.* **2000**, *131*, 412-416.

(24) Khun, N., Liu, E. Effects of platinum content on tribological properties of platinum/nitrogen doped diamond-like carbon thin films deposited via magnetron sputtering. *Friction* **2014**, *2*, 64-72.

(25) Khadem, M., Penkov, O.V., Pukha, V.E., Maleyev, M.V., Kim, D.E. Ultra-thin nano-patterned wear-protective diamond-like carbon coatings deposited on glass using a C60 ion beam. *Carbon* **2014**, *80*, 534-543.

(26) Kaczorowski, W., Szymanski, W., Batory, D., Niedzielski, P. Tribological Properties and Characterization of Diamond Like Carbon Coatings Deposited by MW/RF and RF Plasma-Enhanced CVD Method on Poly(ether-ether-ketone). *Plasma Processes Polym.* **2014**, *11*, 878-887.

(27) Nohava, J., Randall, N.X., Conte, N. Novel ultra nanoindentation method with extremely low thermal drift: Principle and experimental results. *J. Mater. Res.* **2009**, *24*, 873-882.

(28) Randall, N.X., Vandamme, M., Ulm, F.J. Nanoindentation analysis as a two-dimensional tool for mapping the mechanical properties of complex surfaces. *J. Mater. Res.* **2009**, *24*, 679-690.

(29) Stachowiak, G.W. *Wear – materials, mechanisms and practice;* Wiley: San Diego, **2005**.

(30) Kato, K. Wear in relation to friction — a review. *Wear* **2000**, *241*, 151-157.

(31) Gnecco, E., Meyer, E. *Fundamentals of Friction and Wear on the Nanoscale;* Springer-Verlag: Berlin, **2015**.

(32) Budinski, K.G. *Friction, Wear and Errosion Atlas;* CRC Press: Boka Raton, **2014**.

(33) MartinezMartinez, D., De Hosson, J.T. On the deposition and properties of DLC protective coatings on elastomers: A critical review. *Surf. Coat. Technol.* **2014**, *258*, 677-690.

(34) Fan, C., Li, C., Inoue, A., Haas, V. Deformation behavior of Zr-based bulk nanocrystalline amorphous alloys. *Phys. Rev. B.* **2000**, *61*, R3761-R3763.

(35) Krishnan, R., Gupta, H.O., Sella, C., Kaabouchi, M. Magnetic and structural studies in sputtered Ni/C, Co/C and Fe/C multilayers. *J. Magn. Magn. Mater.* **1991**, *93*, 174-178.

(36) Chernov, V.A., Chkhalo, N.I., Fedorchenko, M.V., Kruglyakov, E.P., Mytnichenko, S.V., Nikitenko, S.G. Study of the Inner Structure of Co/C and Ni/C Multilayers Prepared by Pulsed Laser Evaporation Method. *J. X-ray Sci. Technol.* **1995**, *5*, 65-72.

(37) Liqin, L., Zhanshan, W., Jingtao, Z., Zhong, Z., Moyan, T., Qiushi, H., Rui, C., Jing, X., Lingyan, C. Intrinsic stress analysis of sputtered carbon film. *Chin. Opt. Lett.* **2008**, *6*, 384-385.

(38) Johnson, K. *Contact mechanics;* Cambridge University Press: Cambridge, **1985**.